J. Fluid Mech. (2012), *vol.* 705, *pp.* 120–133.
doi:10.1017/jfm.2011.484

Viscous Marangoni propulsion

Eric Lauga† and Anthony M. J. Davis

Department of Mechanical and Aerospace Engineering, University of California, San Diego, 9500 Gilman Drive, La Jolla, CA 92093-0411, USA

(Received 3 May 2011; revised 15 October 2011; accepted 1 November 2011; first published online 19 December 2011)

Marangoni propulsion is a form of locomotion wherein an asymmetric release of surfactant by a body located at the surface of a liquid leads to its directed motion. We present in this paper a mathematical model for Marangoni propulsion in the viscous regime. We consider the case of a thin rigid circular disk placed at the surface of a viscous fluid and whose perimeter has a prescribed concentration of an insoluble surfactant, to which the rest of its surface is impenetrable. Assuming a linearized equation of state between surface tension and surfactant concentration, we derive analytically the surfactant, velocity and pressure fields in the asymptotic limit of low capillary, Péclet and Reynolds numbers. We then exploit these results to calculate the Marangoni propulsion speed of the disk. Neglecting the stress contribution from Marangoni flows is seen to over-predict the propulsion speed by 50 %.

Key words: capillary flows, low-Reynolds-number flows, propulsion

1. Introduction

The study of animal locomotion, as carried out by zoologists and organismal biologists (Gray 1968; Alexander 2002*b*), has long been a source of new problems in fluid dynamics, either because fluid flows pose biological constraints which deserve to be quantified (Vogel 1996) or because biological situations lead to interesting and new fluid physics (Lighthill 1975; Childress 1981). Broadly speaking, there exist two types of self-propelled motion in fluids. In the first type, locomotion is induced by shape changes. This category includes all classical biologically relevant work at both high and low Reynolds numbers, and encompasses flying birds (Alexander 2002*a*) and insects (Maxworthy 1981; Ellington 1984; Alexander 2002*a*; Wang 2005), swimming fish (Lighthill 1975; Triantafyllou, Triantafyllou & Yue 2000; Fish & Lauder 2006), the locomotion of microorganisms (Brennen & Winet 1977; Pedley & Kessler 1992; Fauci & Dillon 2006; Lauga & Powers 2009) and interfacial propulsion (Bush & Hu 2006).

The second class of self-propulsion is one where motion occurs without relative movement between the body and the fluid. In that case, transport arises due to specific interactions between the body and its surrounding environment. Beyond the trivial case of force-driven motion such as sedimentation (Batchelor 1972), this category includes transport driven by gradients, either externally applied (Young, Goldstein & Block 1959; Barton & Subramanian 1989; Brochard 1989; Chaudhury & Whitesides 1992)

† Email address for correspondence: elauga@ucsd.edu

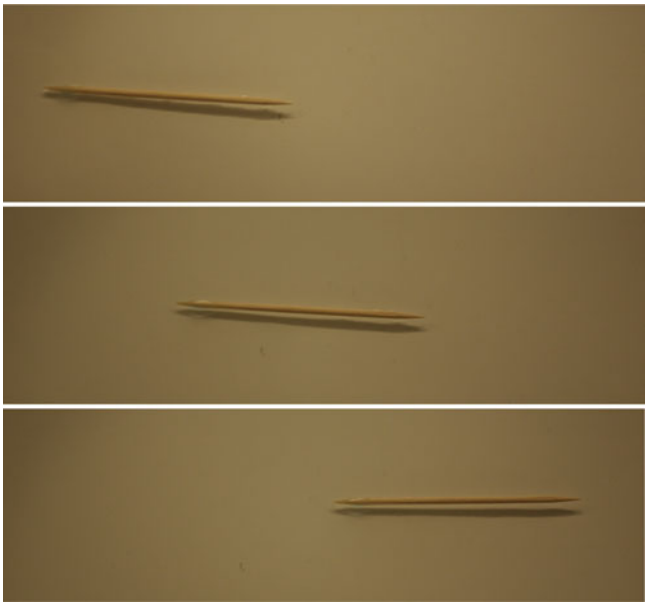

FIGURE 1. (Colour online available at journals.cambridge.org/flm) Example of Marangoni propulsion in the kitchen sink. The tip of a toothpick is dipped in dishwasher liquid, and is then deposited at the free surface of a water container. The surface tension at the contact line near the rear of the toothpick is smaller than that near the front, leading to forward propulsion. The toothpick length is 6.5 cm.

or self-generated (Paxton *et al.* 2004; Golestanian, Liverpool & Ajdari 2005; Paxton *et al.* 2006; Howse *et al.* 2007; Ruckner & Kapral 2007). In this paper, we consider a specific setup belonging to this second category, namely locomotion at the surface of a liquid driven by self-generated surface tension gradients, a situation sometimes referred to as Marangoni propulsion (Bush & Hu 2006).

A gradient in surface tension at the surface of a liquid can give rise to transport for two distinct physical reasons. First, surface tension acts as a force along contact lines. A body subject to a surface tension gradient with non-zero average will thus experience a net force, and will have to move. Well-studied examples include droplets moving on substrates with prescribed gradients in surface energy (Greenspan 1978; Brochard 1989; Chaudhury & Whitesides 1992), or reacting with a substrate to self-generate similar asymmetries (Bain, Burnetthall & Montgomerie 1994; Dossantos & Ondarcuhu 1995). Surface tension gradients can also lead to transport because of Marangoni flows. The tangential stress condition at the interface between two fluids states that tangential viscous stresses are in mechanical equilibrium with gradients in surface tension, and thus any imbalance in surface tension leads to a flow (Scriven & Sternling 1960). Examples of Marangoni transport include the motion of droplets and bubbles in thermal gradients (Young *et al.* 1959; Barton & Subramanian 1989; Brochard 1989) and droplets subject to internal releases of surfactant (Tsemakh, Lavrenteva & Nir 2004).

Marangoni propulsion refers to the situation where a body, located at the surface of a fluid, generates an asymmetric distribution of surface active materials, thereby prompting a surface tension imbalance and a Marangoni flow, both of which lead to locomotion. A simple illustration of this phenomenon is displayed in figure 1 using

a toothpick dipped in a low-surface-tension dishwasher liquid. The surface tension at the contact line near the rear of the toothpick is smaller than that near the front, which leads to forward propulsion. Marangoni propulsion in nature, recently reviewed by Bush & Hu (2006), is of relevance to the behaviour of insects. The most studied is *Stenus* (rove beetle), which is observed to recover from a fall on a water surface by quickly releasing surface active materials (Billard & Bruylant 1905; Joy 1910; Linsenmair & Jander 1963; Schildknecht 1976; Betz 2002). Marangoni locomotion is also used by *Dianous* (rove beetle) (Jenkins 1960) and *Velia* (small water strider) (Linsenmair & Jander 1963).

Experimentally, a lot of work has been carried out on synthetic Marangoni propulsion, mostly regarding the dynamics of so-called camphor boats, where the dissolution of camphor grains at the surface of water leads to their propulsion (Rayleigh 1890; Nakata *et al.* 1997). For that system, the Marangoni flow has been visualized (Kitahata *et al.* 2004), and one-dimensional modelling has been proposed (Kohira *et al.* 2001; Kitahata *et al.* 2004). The combination of a chemical and hydrodynamic field has further been found to lead to interesting coupling between different bodies (Kohira *et al.* 2001; Soh, Bishop & Grzybowski 2008), and between bodies and boundaries (Nakata, Doi & Kitahata 2004). Similar physics dictates the motion of camphanic acid boats (Nakata & Kirisaka 2006; Nakata *et al.* 2006), phenanthroline disks (Nakata & Arima 2008; Iida *et al.* 2010), ethanol-soaked gels on water surface (Bassik, Abebe & Gracias 2008) and mercury drops near oxidant crystals (Nakata *et al.* 2000).

In this paper we consider what is perhaps the simplest model of Marangoni propulsion, namely the case of a thin circular rigid disk located at the surface of a viscous fluid (§ 2). We assume that a portion of the perimeter of the disk has a prescribed concentration of insoluble surfactant, to which the rest of the disk surface is impenetrable. Assuming a linearized equation of state between surface tension and the concentration of surfactant, we derive mathematically in § 3 in the limit of low capillary, Péclet and Reynolds numbers the surfactant concentration field (§ 3.1), the fluid velocity and pressure fields (§ 3.2) and the propulsion speed of the disk (§ 3.3). Our results, and the regime in which all our assumptions are expected to be valid, are summarized in § 4. In particular, we show that neglecting the viscous stresses acting on the disk as a result of Marangoni flows over-predicts the propulsion speed by 50 %.

2. Model problem and setup

The model problem we consider in this paper is illustrated in figure 2. A solid disk of radius a lies in the horizontal surface of an otherwise unbounded, viscous, incompressible fluid whose coefficient of viscosity is μ. Fluid motion and edgewise translation of the disk are induced by a non-uniform surface distribution of an insoluble surfactant, of concentration Γ per unit area. Specifically, the rear part of the disk (the arc described by $|\phi|$ between α and π, where ϕ is the polar angle in cylindrical coordinates) is assumed to have a prescribed concentration of surfactant, described by $f(|\phi|)$ in a dimensionless form. The front part of the disk ($|\phi|$ between 0 and α) is impenetrable to the surfactant and thus the normal derivative of Γ is zero on this circular arc. The surfactant is assumed to be insoluble in the fluid, and thus we ignore its transport to and from the bulk. For a water–air interface, this would be an appropriate approximation for surfactants such as oleyl alcohol or hemicyanine (Phongikaroon *et al.* 2005), and more generally organic compounds with long-chain hydrocarbon tails and polar hydrophilic heads (Tsai & Yue 1995).

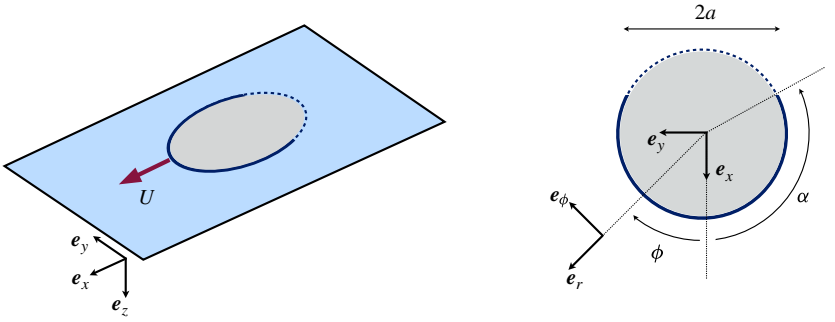

FIGURE 2. (Colour online) Setup for our model of viscous Marangoni propulsion. A solid disk of radius a is located at the surface of a semi-infinite fluid of viscosity μ. The front part of the disk ($|\phi|$ between 0 and α in polar coordinates) is assumed to be impermeable to surfactants. The rear part of the disk ($|\phi|$ between α and π) is assumed to have a prescribed concentration of insoluble surfactant, described by $f(|\phi|)$ in a dimensionless form, leading to forward propulsion of the disk at speed U. The free surface is assumed to be undeformed by the motion of the disk, and remains flat (limit of small capillary numbers). The Péclet number for the surfactant is small enough to neglect all convective terms in the surfactant transport equation, while the Reynolds number in the fluid is small enough for the fluid motion to be described by Stokes flow.

Provided we consider this problem after the initial transient in fluid flow and surfactant transport, the governing steady-state equation for surfactant concentration at the free surface (Stone 1990) is given by

$$D\nabla_s^2\Gamma = \boldsymbol{\nabla}\cdot(\boldsymbol{v}_s\Gamma), \tag{2.1}$$

where D is the diffusion coefficient and $\boldsymbol{v}_s$ is the surface component of the fluid velocity $\boldsymbol{v}$. This latter satisfies the continuity equation,

$$\boldsymbol{\nabla}\cdot\boldsymbol{v} = 0, \tag{2.2}$$

and is assumed to be sufficiently small not only to allow use of the Stokes equations,

$$\mu\nabla^2\boldsymbol{v} = \boldsymbol{\nabla}p, \tag{2.3}$$

where p is the dynamic pressure, but also to furnish a zero Péclet number approximation to the surfactant field, Γ_0, by neglecting the right-hand side of (2.1). In addition, the fluid surface is assumed to remain flat. In other words, we focus in this paper on the limit where all three Reynolds, Péclet and capillary numbers are asymptotically small; an *a posteriori* derivation of the conditions under which these limits are valid is offered in § 4. The zero Péclet number surfactant field Γ_0, satisfies Laplace's equation, and is fully determined by its prescribed values at the disk (§ 3.1). The resulting Marangoni stresses induce the lowest approximation to $\boldsymbol{v}$ (§ 3.2), which enables the translation speed of the disk to be determined (§ 3.3). We use cylindrical polar coordinates (ar, ϕ, az), with the origin at the centre of the disk and z measured vertically downwards (see figure 2). In what follows, both r and z are thus dimensionless.

3. Analysis

3.1. *Surfactant concentration*

Being a solution of the two-dimensional Laplace's equation, the surfactant concentration, Γ_0, in the surface $z = 0$, exterior to the disk, is of the form

$$\Gamma_0 a^2 = c_0 + 2\sum_{n=1}^{\infty} c_n r^{-n} \cos n\phi \quad (r > 1). \tag{3.1}$$

The dimensionless coefficients $\{c_n; n \geqslant 0\}$ are determined by the mixed boundary conditions,

$$\Gamma_0 a^2 = f(|\phi|) \text{ at } r = 1 \quad (\alpha < |\phi| < \pi), \tag{3.2a}$$

$$\frac{\partial \Gamma_0}{\partial r} = 0 \text{ at } r = 1 \quad (0 < |\phi| < \alpha), \tag{3.2b}$$

in which f is a prescribed, non-constant function that is symmetric with respect to the $\phi = \pm\pi$ direction. Application of (3.2*a*) and (3.2*b*) to (3.1) yields a mixed boundary value problem involving cosine series, namely,

$$c_0 + 2\sum_{n=1}^{\infty} c_n \cos n\phi = f(\phi) \quad (\alpha < \phi \leqslant \pi), \tag{3.3a}$$

$$\sum_{n=1}^{\infty} n c_n \cos n\phi = 0 \quad (0 \leqslant \phi < \alpha). \tag{3.3b}$$

Following the method given by Sneddon (1966) (§ 5.4.3), we set

$$c_0 + 2\sum_{n=1}^{\infty} c_n \cos n\phi = \cos\frac{1}{2}\phi \int_{\phi}^{\alpha} \frac{h(t)\,\mathrm{d}t}{\sqrt{\cos\phi - \cos t}} \quad (0 \leqslant \phi < \alpha), \tag{3.4}$$

which extends the range of (3.3*a*) to the complementary interval by using an Abel transform in anticipation of the $\sqrt{\alpha - \phi}$ behaviour as $\phi \to \alpha$ from below. This immediately yields the Fourier coefficients

$$c_n = \frac{1}{\pi}\left[\int_0^{\alpha} \cos\frac{1}{2}v \int_v^{\alpha} \frac{h(t)\,\mathrm{d}t}{\sqrt{\cos v - \cos t}} \cos nv\,\mathrm{d}v + \int_{\alpha}^{\pi} f(v)\cos nv\,\mathrm{d}v\right] \quad (n \geqslant 0). \tag{3.5}$$

When (3.5) is substituted into (3.1), the summations can be evaluated in closed form; but first we need to relate $h(t)$ to $f(\phi)$.

A change in the order of integration in (3.5) yields

$$c_n = \frac{1}{\pi}\left[\int_0^{\alpha} h(t)\,\mathrm{d}t \int_0^{t} \frac{\cos\frac{1}{2}v \cos nv\,\mathrm{d}v}{\sqrt{\cos v - \cos t}} + \int_{\alpha}^{\pi} f(v)\cos nv\,\mathrm{d}v\right] \quad (n \geqslant 0). \tag{3.6}$$

When these coefficients are substituted into the integral of (3.3*b*) between 0 and ϕ – the integration constant being trivially zero – the common summation can be evaluated and the double integral reduced to a single integral, giving the Abel integral equation,

$$\int_0^{\phi} \frac{h(t)\,\mathrm{d}t}{\sqrt{\cos t - \cos\phi}} = \frac{2}{\pi}\sin\frac{1}{2}\phi \int_{\alpha}^{\pi} \frac{f(v)\,\mathrm{d}v}{\cos\phi - \cos v} \quad (0 \leqslant \phi \leqslant \alpha). \tag{3.7}$$

Inversion then gives, after evaluating the t-integral,

$$h(t) = \frac{2}{\pi}\frac{\mathrm{d}}{\mathrm{d}t}\int_\alpha^\pi \frac{f(v)\sin\frac{1}{2}v}{\sqrt{\cos t - \cos v}}\,\mathrm{d}v \quad (0 \leqslant t \leqslant \alpha). \tag{3.8}$$

The first two coefficients are thus given, from (3.6), by

$$c_0 = \frac{1}{\sqrt{2}}\int_0^\alpha h(t)\,\mathrm{d}t + \frac{1}{\pi}\int_\alpha^\pi f(v)\,\mathrm{d}v = \frac{\sqrt{2}}{\pi}\int_\alpha^\pi \frac{f(v)\sin\frac{1}{2}v}{\sqrt{\cos\alpha - \cos v}}\,\mathrm{d}v, \tag{3.9}$$

$$\begin{aligned} c_1 &= \frac{1}{\sqrt{2}}\int_0^\alpha h(t)\cos^2\frac{1}{2}t\,\mathrm{d}t + \frac{1}{\pi}\int_\alpha^\pi f(v)\cos v\,\mathrm{d}v \\ &= \frac{1}{\pi\sqrt{2}}\int_\alpha^\pi \frac{f(v)\sin\frac{1}{2}v}{\sqrt{\cos\alpha - \cos v}}(1 - \cos\alpha + 2\cos v)\,\mathrm{d}v. \end{aligned} \tag{3.10}$$

More significantly, the solution (3.8) enables the integral in (3.5) to be expressed in terms of the prescribed $f(\phi)$ by evaluating the t-integral to give

$$\int_u^\alpha \frac{h(t)\,\mathrm{d}t}{\sqrt{\cos u - \cos t}} = \frac{2}{\pi}\int_\alpha^\pi \frac{f(v)\sin\frac{1}{2}v\,\mathrm{d}v}{\cos u - \cos v}\sqrt{\frac{\cos u - \cos\alpha}{\cos\alpha - \cos v}} \quad (0 < u < \alpha). \tag{3.11}$$

Now the substitution of (3.5) into (3.1) and evaluation of the summations yields a closed-form expression for the surfactant distribution, namely,

$$\begin{aligned} \Gamma_0 a^2 = {} & \frac{1}{2\pi}\int_\alpha^\pi f(v)\left[\frac{r^2-1}{r^2+1-2r\cos(\phi+v)} + \frac{r^2-1}{r^2+1-2r\cos(\phi-v)}\right]\mathrm{d}v \\ & + \frac{1}{\pi^2}\int_0^\alpha \cos\frac{1}{2}u\int_\alpha^\pi \frac{f(v)\sin\frac{1}{2}v}{\cos u - \cos v}\sqrt{\frac{\cos u - \cos\alpha}{\cos\alpha - \cos v}}\,\mathrm{d}v \\ & \times\left[\frac{r^2-1}{r^2+1-2r\cos(\phi+u)} + \frac{r^2-1}{r^2+1-2r\cos(\phi-u)}\right]\mathrm{d}u, \end{aligned} \tag{3.12}$$

valid for $r \geqslant 1$. Note that the case where $f(\phi) = f_0$, a constant, yields a uniform surfactant concentration around the disk edge, and hence no asymmetry to generate motion.

3.2. *Pressure and velocity field*

The Marangoni stresses induce a fluid motion via the boundary condition for tangential stresses

$$\mu\frac{\partial \boldsymbol{v}_s}{\partial z} = -\boldsymbol{\nabla}_s\gamma = \mathscr{R}T_A\boldsymbol{\nabla}_s\Gamma_0, \tag{3.13}$$

where γ is the surface tension, $\mathscr{R}$ is the gas constant, T_A is the absolute temperature, and the linearized equation of state, $\gamma = \gamma_0 - \mathscr{R}T_A\Gamma$ (Gibbs 1878; Pawar & Stebe 1996), is invoked.

The pressure p has the Fourier mode expansion,

$$p = P_0(r,z) + 2\sum_{n=1}^{\infty} P_n(r,z)\cos n\phi, \tag{3.14}$$

in which, since (2.2) and (2.3) imply that p is Laplacian, the coefficients have Hankel transforms of type

$$P_n = \frac{2\mu}{a}\int_0^\infty kA_n(k)\mathrm{e}^{-kz}\mathrm{J}_n(kr)\,\mathrm{d}k \quad (n \geqslant 0). \tag{3.15}$$

It is then advantageous to write the velocity field in the form

$$\begin{aligned}\boldsymbol{v} = {} & \boldsymbol{e}_r S_0(r,z) + \sum_{n=1}^{\infty}[\boldsymbol{e}_r\cos n\phi + \boldsymbol{e}_\phi \sin n\phi]S_n(r,z) \\ & + \sum_{n=1}^{\infty}[\boldsymbol{e}_r\cos n\phi - \boldsymbol{e}_\phi \sin n\phi]Q_n(r,z) \\ & + \boldsymbol{e}_z\left[W_0(r,z) + 2\sum_{n=1}^{\infty}W_n(r,z)\cos n\phi\right].\end{aligned} \tag{3.16}$$

This ensures that the modal structure is preserved on substitution, with (3.14), into (2.3), which gives

$$\begin{aligned}& \boldsymbol{e}_r\left(\frac{\partial^2}{\partial r^2} + \frac{1}{r}\frac{\partial}{\partial r} - \frac{1}{r^2} + \frac{\partial^2}{\partial z^2}\right)S_0 \\ & \quad + \sum_{n=1}^{\infty}[\boldsymbol{e}_r\cos n\phi + \boldsymbol{e}_\phi\sin n\phi]\left[\frac{\partial^2}{\partial r^2} + \frac{1}{r}\frac{\partial}{\partial r} - \frac{(n+1)^2}{r^2} + \frac{\partial^2}{\partial z^2}\right]S_n \\ & \quad + \sum_{n=1}^{\infty}[\boldsymbol{e}_r\cos n\phi - \boldsymbol{e}_\phi\sin n\phi]\left[\frac{\partial^2}{\partial r^2} + \frac{1}{r}\frac{\partial}{\partial r} - \frac{(n-1)^2}{r^2} + \frac{\partial^2}{\partial z^2}\right]Q_n \\ & \quad + \boldsymbol{e}_z\left[\left(\frac{\partial^2}{\partial r^2} + \frac{1}{r}\frac{\partial}{\partial r} + \frac{\partial^2}{\partial z^2}\right)W_0 + 2\sum_{n=1}^{\infty}\left(\frac{\partial^2}{\partial r^2} + \frac{1}{r}\frac{\partial}{\partial r} - \frac{n^2}{r^2} + \frac{\partial^2}{\partial z^2}\right)W_n\cos n\phi\right] \\ & = \frac{a}{\mu}\left[\boldsymbol{e}_r\frac{\partial P_0}{\partial r} + \sum_{n=1}^{\infty}[\boldsymbol{e}_r\cos n\phi + \boldsymbol{e}_\phi\sin n\phi]\left(\frac{\partial P_n}{\partial r} - \frac{n}{r}P_n\right)\right. \\ & \quad + \sum_{n=1}^{\infty}[\boldsymbol{e}_r\cos n\phi - \boldsymbol{e}_\phi\sin n\phi]\left(\frac{\partial P_n}{\partial r} + \frac{n}{r}P_n\right) \\ & \quad \left. + \boldsymbol{e}_z\left(\frac{\partial P_0}{\partial z} + 2\sum_{n=1}^{\infty}\frac{\partial P_n}{\partial z}\cos n\phi\right)\right].\end{aligned} \tag{3.17}$$

With P_n given by (3.15), it readily follows that the three sets of partial differential equations in (3.17) have solutions of the form

$$S_n = \int_0^\infty [D_n(k) + kzA_n(k)]\mathrm{e}^{-kz}\mathrm{J}_{n+1}(kr)\,\mathrm{d}k \quad (n \geqslant 0), \tag{3.18a}$$

$$Q_n = \int_0^\infty [B_n(k) - kzA_n(k)]\mathrm{e}^{-kz}\mathrm{J}_{n-1}(kr)\,\mathrm{d}k \quad (n \geqslant 1), \tag{3.18b}$$

$$W_n = \int_0^\infty kzA_n(k)\mathrm{e}^{-kz}\mathrm{J}_n(kr)\,\mathrm{d}k \quad (n \geqslant 0), \tag{3.18c}$$

in which the complementary function in (3.18*c*) is chosen according to the assumption of no normal flow in the plane ($z = 0$) of the disk and surfactant. Substitution of (3.16) into (2.2) gives

$$\frac{1}{r}\frac{\partial}{\partial r}(rS_0) + \frac{\partial W_0}{\partial z} = 0, \tag{3.19}$$

$$\frac{1}{r^{n+1}}\frac{\partial}{\partial r}(r^{n+1}S_n) + r^{n-1}\frac{\partial}{\partial r}\left(\frac{Q_n}{r^{n-1}}\right) + 2\frac{\partial W_n}{\partial z} = 0 \quad (n \geqslant 1), \tag{3.20}$$

whence

$$D_0(k) + A_0(k) = 0, \quad D_n(k) - B_n(k) + 2A_n(k) = 0 \quad (k > 0, n \geqslant 1). \tag{3.21}$$

These functions are determined by imposing conditions on the tangential velocity components in the plane $z = 0$. The uniform translation of the disk, due to the Marangoni stresses, is expressed by

$$\boldsymbol{v} = U\boldsymbol{e}_x \quad \text{at } z = 0, r < 1, \tag{3.22}$$

where U is to be determined by a subsequent force balance (see § 3.3). When substituted into (3.16), (3.22) implies that

$$Q_1 = U, \quad Q_n = 0 \ (n > 1), \quad S_n = 0 \ (n \geqslant 0) \quad \text{at } z = 0, r < 1. \tag{3.23}$$

As in Davis (1991*a*,*b*), the Bessel functions in (3.18*a*) and (3.18*b*) are changed to J_n by integration with respect to r, aided by the classic recurrence relations (Abramowitz & Stegun 1969). The arbitrary constants that multiply a non-negative power of r are retained and chosen below to eliminate square root singularities in the velocities. Thus our required forms of the integral conditions on the interval $r < 1$ are

$$\int_0^\infty D_n(k)k^{-1}\mathrm{J}_n(kr)\,\mathrm{d}k = d_n r^n \quad (r < 1, n \geqslant 0), \tag{3.24a}$$

$$\int_0^\infty B_n(k)k^{-1}\mathrm{J}_n(kr)\,\mathrm{d}k = \frac{U}{2}r\delta_{1n} \quad (r < 1, n \geqslant 1), \tag{3.24b}$$

where δ_{mn} denotes the Kronecker delta.

Integral conditions on the interval $r > 1$ are obtained by applying the Marangoni stress condition, (3.13). Equation (3.1) shows that only the functions $\{S_n; n \geqslant 0\}$ in (3.16) are directly forced by the surface tension variations in (3.13). Replacing $\mathrm{J}_{n\pm1}$ by J_n as above, our required forms of the integral conditions become

$$\int_0^\infty [D_0(k) - A_0(k)]\mathrm{J}_0(kr)\,\mathrm{d}k = 0 \quad (r > 1), \tag{3.25a}$$

$$\int_0^\infty [D_n(k) - A_n(k)]\mathrm{J}_n(kr)\,\mathrm{d}k = \frac{\mathscr{R}T_A}{\mu a^2}c_n r^{-n} \quad (r > 1, n \geqslant 1), \tag{3.25b}$$

$$\int_0^\infty [B_n(k) + A_n(k)]\mathrm{J}_n(kr)\,\mathrm{d}k = b_n r^{-n} \quad (r > 1, n \geqslant 1). \tag{3.25c}$$

We now use (3.21) to eliminate $\{A_n; n \geqslant 0\}$ from (3.25*a*)–(3.25*c*) and obtain

$$\int_0^\infty D_0(k)\mathrm{J}_0(kr)\,\mathrm{d}k = 0 \quad (r > 1), \tag{3.26a}$$

$$\int_0^\infty D_n(k)\mathrm{J}_n(kr)\,\mathrm{d}k = \left[3\frac{\mathscr{R}T_A}{\mu a^2}c_n + b_n\right]\frac{r^{-n}}{4} \quad (r > 1, n \geqslant 1), \tag{3.26b}$$

$$\int_0^\infty B_n(k)\mathrm{J}_n(kr)\,\mathrm{d}k = \left[\frac{\mathscr{R}T_A}{\mu a^2}c_n + 3b_n\right]\frac{r^{-n}}{4} \quad (r > 1, n \geqslant 1). \tag{3.26c}$$

Equation (3.24*a*) with (3.26*a*), (3.26*b*) and (3.24*b*) with (3.26*c*) define two infinite sets of mixed boundary value problems of a type discussed by Sneddon (1966) (§ 4.3). The continuation of the integrals in (3.24*a*) and (3.24*b*) is given by

$$\int_0^\infty D_0(k)k^{-1}\mathrm{J}_0(kr)\,\mathrm{d}k = \frac{2d_0}{\pi}\int_0^{1/r}\frac{\mathrm{d}u}{\sqrt{1-u^2}} \quad (r>1), \tag{3.27a}$$

$$\int_0^\infty D_n(k)k^{-1}\mathrm{J}_n(kr)\,\mathrm{d}k = \frac{2d_n r^n\Gamma(n+1)}{\Gamma(1/2)\Gamma(n+1/2)}\int_0^{1/r}\frac{u^{2n}\,\mathrm{d}u}{\sqrt{1-u^2}} + \left[3\frac{\mathscr{R}T_A}{\mu a^2}c_n + b_n\right]\frac{\Gamma(n-1/2)\,(r^2-1)^{1/2}}{4\Gamma(1/2)\Gamma(n)r^n} \quad (r>1,\, n\geqslant 1), \tag{3.27b}$$

$$\int_0^\infty B_n(k)k^{-1}\mathrm{J}_n(kr)\,\mathrm{d}k = \frac{2Ur\delta_{1n}}{\pi}\int_0^{1/r}\frac{u^2\,\mathrm{d}u}{\sqrt{1-u^2}} + \left[\frac{\mathscr{R}T_A}{\mu a^2}c_n + 3b_n\right]\frac{\Gamma(n-1/2)\,(r^2-1)^{1/2}}{4\Gamma(1/2)\Gamma(n)r^n} \quad (r>1,\, n\geqslant 1). \tag{3.27c}$$

The arbitrary constants are finally determined by eliminating edge singularities from the surface velocity components. From (3.18*a*) and (3.27*a*), we have

$$\begin{aligned} S_0(r,0) &= \int_0^\infty D_0(k)\mathrm{J}_1(kr)\,\mathrm{d}k = -\frac{\mathrm{d}}{\mathrm{d}r}\int_0^\infty D_0(k)k^{-1}\mathrm{J}_0(kr)\,\mathrm{d}k \\ &= -\frac{2d_0}{\pi}\frac{\mathrm{d}}{\mathrm{d}r}\arcsin\left(\frac{1}{r}\right) = 0 \quad (r>1), \end{aligned} \tag{3.28}$$

provided that $d_0 = 0$.

From (3.18*a*) and (3.27*b*),

$$\begin{aligned} S_n(r,0) &= \int_0^\infty D_n(k)\mathrm{J}_{n+1}(kr)\,\mathrm{d}k = -r^n\frac{\mathrm{d}}{\mathrm{d}r}\left[\frac{1}{r^n}\int_0^\infty D_n(k)k^{-1}\mathrm{J}_n(kr)\,\mathrm{d}k\right] \\ &= \frac{2d_n\Gamma(n+1)}{\Gamma(1/2)\Gamma(n+1/2)}\frac{r^{-(n+1)}}{(r^2-1)^{1/2}} \\ &\quad - \left[3\frac{\mathscr{R}T_A}{\mu a^2}c_n + b_n\right]\frac{r^n\Gamma(n-1/2)}{4\Gamma(1/2)\Gamma(n)}\frac{\mathrm{d}}{\mathrm{d}r}\left[\frac{(r^2-1)^{1/2}}{r^{2n}}\right] \\ &= \left[3\frac{\mathscr{R}T_A}{\mu a^2}c_n + b_n\right]\frac{\Gamma(n+1/2)}{2\Gamma(1/2)\Gamma(n)}\frac{(r^2-1)^{1/2}}{r^{n+1}} \quad (r>1,\, n\geqslant 1), \end{aligned} \tag{3.29}$$

provided that

$$\frac{2d_n\Gamma(n+1)}{\Gamma(1/2)\Gamma(n+1/2)} = \left[3\frac{\mathscr{R}T_A}{\mu a^2}c_n + b_n\right]\frac{\Gamma(n-1/2)}{4\Gamma(1/2)\Gamma(n)} \quad (n\geqslant 1). \tag{3.30}$$

From (3.18*b*) and (3.27*c*),

$$\begin{aligned} Q_n(r,0) &= \int_0^\infty B_n(k)\mathrm{J}_{n-1}(kr)\,\mathrm{d}k = \frac{1}{r^n}\frac{\mathrm{d}}{\mathrm{d}r}\left[r^n\int_0^\infty B_n(k)k^{-1}\mathrm{J}_n(kr)\,\mathrm{d}k\right] \\ &= \frac{2U}{\pi}\delta_{1n}\arcsin\left(\frac{1}{r}\right) \quad (r>1,\, n\geqslant 1), \end{aligned} \tag{3.31}$$

provided that

$$\frac{\mathscr{R}T_A}{\mu a^2}c_n + 3b_n = \frac{8U}{\pi}\delta_{1n} \quad (n \geqslant 1). \tag{3.32}$$

On using (3.30) and (3.32) to eliminate the coefficients $\{d_n, b_n; n \geqslant 1\}$, the surface velocity is given from (3.16) by

$$\boldsymbol{v}_s = \frac{2U}{\pi}\left[\arcsin\left(\frac{1}{r}\right)(\boldsymbol{e}_r\cos\phi - \boldsymbol{e}_\phi\sin\phi) + \frac{(r^2-1)^{1/2}}{3r^2}(\boldsymbol{e}_r\cos\phi + \boldsymbol{e}_\phi\sin\phi)\right]$$
$$+ \frac{4\mathscr{R}T_A}{3\mu a^2}\sum_{n=1}^{\infty} c_n[\boldsymbol{e}_r\cos n\phi + \boldsymbol{e}_\phi\sin n\phi]\frac{\Gamma(n+1/2)}{\Gamma(1/2)\Gamma(n)}\frac{(r^2-1)^{1/2}}{r^{n+1}} \quad (r>1). \tag{3.33}$$

Note that $\boldsymbol{v}_s = U\boldsymbol{e}_x + O[(r^2-1)^{1/2}]$ as $r \to 1+$, giving the expected continuous velocities. The summation in (3.33) can be expressed as

$$(r^2-1)^{1/2}\,\nabla\left[-\sum_{n=1}^{\infty} c_n r^{-n}\cos n\phi\frac{\Gamma(n+1/2)}{\Gamma(1/2)\Gamma(n+1)}\right] \quad (r>1), \tag{3.34}$$

and then, by reference to $(1-x)^{-1/2}$, evaluated as in (3.12).

3.3. *Marangoni propulsion speed*

The disk speed U is found by enforcing that the viscous drag force,

$$2\pi\mu\boldsymbol{e}_x\int_0^1 \frac{\partial Q_1}{\partial z}(r,0)r\,\mathrm{d}r = -2\pi\mu\boldsymbol{e}_x\int_0^\infty [B_1(k)+A_1(k)]\mathrm{J}_1(k)\,\mathrm{d}k, \tag{3.35}$$

is balanced by the force on the disk due to surface tension,

$$\boldsymbol{e}_x\int_{-\pi}^{\pi}(\gamma)_{r=1}\cos\phi\,\mathrm{d}\phi = -2\pi\boldsymbol{e}_x\frac{\mathscr{R}T_A}{a^2}c_1, \tag{3.36}$$

in which (3.16), (3.18*b*), (3.13), (3.1) have been used (recall that c_1 is given explicitly by (3.10)). Thus U is determined by the equality

$$\int_0^\infty [B_1(k)+A_1(k)]\mathrm{J}_1(k)\,\mathrm{d}k = -\frac{\mathscr{R}T_A}{\mu a^2}c_1. \tag{3.37}$$

The continuation of the integral in (3.25*c*) is given, for $n=1$, by

$$\int_0^\infty [B_1(k)+A_1(k)]\mathrm{J}_1(kr)\,\mathrm{d}k = \frac{(3U-2d_1)r}{\pi(1-r^2)^{1/2}} + \frac{b_1}{r}\left[1-\frac{1}{(1-r^2)^{1/2}}\right]$$
$$= \frac{1}{3r}\left[\frac{8U}{\pi} - \frac{\mathscr{R}T_A}{\mu a^2}c_1\right][1-(1-r^2)^{1/2}] \quad (r<1), \tag{3.38}$$

and substitution into (3.37) allows us to obtain the final expression for the Marangoni propulsion speed as

$$U = -\frac{\pi\mathscr{R}T_A}{4\mu a^2}c_1. \tag{3.39}$$

For the particular case of $f(\phi) = -\cos\phi$, we get, on substitution in (3.9), (3.10),

$$c_0 = \tfrac{1}{2}(1-\cos\alpha), \quad c_1 = -\tfrac{1}{8}(1+\cos\alpha)^2. \tag{3.40}$$

The positive surfactant concentration at the rear of the disk induces a lower surface tension there and hence a positive speed U. Note the limit values, $c_0(0) = 0$ and $c_1(0) = -1/2$, corresponding to $\Gamma a^2 = -r^{-1}\cos\phi$ in (3.1). Also $c_0(\pi) = 1$ and $c_1(\pi) = 0$, corresponding to a uniform surfactant of magnitude $f(\pi)$, which is the $\alpha \to \pi$ limit of (3.9). Similarly, the particular choice $f(\phi) = \cos 2\phi$ yields $c_1 = -1/4(1 + \cos\alpha)\sin^2\alpha$, while $f(\phi) = -\cos 3\phi$ yields $c_1 = -3/32(1 + \cos\alpha)(1 - 5\cos\alpha)\sin^2\alpha$.

4. Discussion

In this paper we consider a simple model setup for Marangoni propulsion: a thin rigid circular disk located at the flat free surface of a viscous fluid and releasing insoluble surfactants with a prescribed concentration along its edge. As seen above, although both the geometry and setup are quite simple, the mathematical details of the derivation can be quite involved, and point to the richness of the physical problem. Physically, in order for the disk to move with finite speed, (3.39) shows that the surfactant concentration cannot be uniform. From a thermodynamic point of view, the disk motion is thus an intrinsically non-equilibrium effect, where a non-uniform surfactant chemical potential needs to be maintained along the disk edge to drive the Marangoni propulsion.

The steady-state analysis in the paper makes three distinct physical assumptions, namely the limit of small capillary, Péclet and Reynolds numbers. The result for the propulsion speed, (3.39), allows us to derive the appropriate velocity scale for the fluid, namely $U \sim \mathscr{R}T_A c_1/\mu a^2$. With a natural length scale $L \sim a$, we can then use this result to derive the regime under which our three assumptions are expected to be correct, namely

$$Ca = \frac{\mu U}{\gamma_0} = \frac{\mathscr{R}T_A c_1}{\gamma_0 a^2} \ll 1, \tag{4.1a}$$

$$Pe = \frac{Ua}{D} = \frac{\mathscr{R}T_A c_1}{\mu a D} \ll 1, \tag{4.1b}$$

$$Re = \frac{\rho U a}{\nu} = \frac{\rho \mathscr{R}T_A c_1}{\mu^2 a} \ll 1. \tag{4.1c}$$

An interesting observation from our theoretical results concerns the role of Marangoni stresses on the disk motion. An approximate method to derive (3.39) would consist in neglecting the stresses on the disk arising from Marangoni flow. In that case, U would be obtained by balancing the direct forcing from surface tension at the contact line, $F = -2\pi\mathscr{R}T_A c_1/a$ ((3.36), with c_1 from (3.10)) by the viscous drag on the bottom half of the disk, $F = 16\mu a U/3$ (Kim & Karilla 1991), leading to propulsion at the speed $U = -3\pi\mathscr{R}T_A c_1/8\mu a^2$. This result, although it has the correct sign and order of magnitude, actually over-predicts the propulsion speed (3.39) by 50 % and thus both direct surface tension forcing at the contact line and Marangoni flow play important roles in determining the steady-state Marangoni propulsion speed.

Acknowledgements

This work was supported in part by the National Science Foundation (CAREER Grant CBET-0746285 to E.L.).

REFERENCES

ABRAMOWITZ, M. & STEGUN, I. A. 1969 *Handbook of Mathematical Functions*. Dover.

ALEXANDER, D. E. 2002*a* *Nature's Flyers: Birds, Insects, and the Biomechanics of Flight*. The Johns Hopkins University Press.

ALEXANDER, R. M. 2002*b* *Principles of Animal Locomotion*. Princeton University Press.

BAIN, C. D., BURNETTHALL, G. D. & MONTGOMERIE, R. R. 1994 Rapid motion of liquid drops. *Nature* **372**, 414–415.

BARTON, K. D. & SUBRAMANIAN, R. S. 1989 The migration of liquid-drops in a vertical temperature-gradient. *J. Colloid Interface Sci.* **133**, 211–222.

BASSIK, N., ABEBE, B. T. & GRACIAS, D. H. 2008 Solvent driven motion of lithographically fabricated gels. *Langmuir* **24**, 12158–12163.

BATCHELOR, G. K. 1972 Sedimentation in a dilute dispersion of spheres. *J. Fluid Mech.* **52**, 245–268.

BETZ, O. 2002 Performance and adaptive value of tarsal morphology in rove beetles of the genus Stenus (Coleoptera, Staphylinidae). *J. Expl Biol.* **205**, 1097–1113.

BILLARD, G. & BRUYLANT, C. 1905 Sur un mode particulier de locomotion de certains *stenus*. *C. R. Soc. Biol.* **59**, 102–103.

BRENNEN, C. & WINET, H. 1977 Fluid mechanics of propulsion by cilia and flagella. *Annu. Rev. Fluid Mech.* **9**, 339–398.

BROCHARD, F. 1989 Motions of droplets on solid surfaces induced by chemical or thermal gradients. *Langmuir* **5**, 432–438.

BUSH, J. W. M. & HU, D. L. 2006 Walking on water: biolocomotion at the interface. *Annu. Rev. Fluid Mech.* **38**, 339–369.

CHAUDHURY, M. K. & WHITESIDES, G. M. 1992 How to make water run uphill. *Science* **256**, 1539–1541.

CHILDRESS, S. 1981 *Mechanics of Swimming and Flying*. Cambridge University Press.

DAVIS, A. M. J. 1991*a* Shear-flow disturbance due to a hole in the plane. *Phys. Fluids* **3**, 478–480.

DAVIS, A. M. J. 1991*b* Slow viscous flow due to motion of an annular disk: pressure-driven extrusion through an annular hole in a wall. *J. Fluid Mech.* **231**, 51–71.

DOSSANTOS, D. F. & ONDARCUHU, T. 1995 Free-running droplets. *Phys. Rev. Lett.* **75**, 2972–2975.

ELLINGTON, C. P 1984 *The Aerodynamics of Hovering Insect Flight*. The Royal Society.

FAUCI, L. J. & DILLON, R. 2006 Biofluidmechanics of reproduction. *Annu. Rev. Fluid Mech.* **38**, 371–394.

FISH, F. E. & LAUDER, G. V. 2006 Passive and active flow control by swimming fishes and mammals. *Annu. Rev. Fluid Mech.* **38**, 193–224.

GIBBS, J. W. 1878 On the equilibrium of heterogeneous substances. Trans. Conn. Acad. **3**, 343. In *Scientific Papers*, vol. 1 (1961), p. 272. Dover.

GOLESTANIAN, R., LIVERPOOL, T. B. & AJDARI, A. 2005 Propulsion of a molecular machine by asymmetric distribution of reaction products. *Phys. Rev. Lett.* **94**, 220801.

GRAY, J. 1968 *Animal Locomotion*. Norton.

GREENSPAN, H. P. 1978 On the motion of a small viscous droplet that wets a surface. *J. Fluid Mech.* **84**, 125–143.

HOWSE, J. R., JONES, R. A. L., RYAN, A. J., GOUGH, T., VAFABAKHSH, R. & GOLESTANIAN, R. 2007 Self-motile colloidal particles: from directed propulsion to random walk. *Phys. Rev. Lett.* **99**, 048102.

IIDA, K., SUEMATSU, N. J., MIYAHARA, Y., KITAHATA, H., NAGAYAMA, M. & NAKATA, S. 2010 Experimental and theoretical studies on the self-motion of a phenanthroline disk coupled with complex formation. *Phys. Chem. Chem. Phys.* **12**, 1557–1563.

JENKINS, M. F. 1960 On the method by which *Stenus* and *Dianous* (Coleoptera: Staphylinidae) return to the banks of a pool. *Trans. R. Ent. Soc. Lond.* **112**, 1–14.

JOY, N. H. 1910 The behaviour of coleoptera in time of floods. *Trans. Ent. Soc. Lond.* **58**, 379–385.

KIM, S. & KARILLA, J. S. 1991 *Microhydrodynamics: Principles and Selected Applications*. Butterworth-Heinemann.

KITAHATA, H., HIROMATSU, S.-I., DOI, Y., NAKATA, S. & RAFIQUL ISLAM, M. 2004 Self-motion of a camphor disk coupled with convection. *Phys. Chem. Chem. Phys.* **6**, 2409–2414.

KOHIRA, M. I., HAYASHIMA, Y., NAGAYAMA, M. & NAKATA, S. 2001 Synchronized self-motion of two camphor boats. *Langmuir* **17**, 7124–7129.

LAUGA, E. & POWERS, T. R. 2009 The hydrodynamics of swimming microorganisms. *Rep. Prog. Phys.* **72**, 096601.

LIGHTHILL, J. L. 1975 *Mathematical Biofluiddynamics*. SIAM.

LINSENMAIR, K. E. & JANDER, R. 1963 Das Entspannungsschwimmen von *Velia* und *Stenus*. *Naturwissenschaften* **50**, 231.

MAXWORTHY, T. 1981 The fluid dynamics of insect flight. *Annu. Rev. Fluid Mech.* **13**, 329–350.

NAKATA, S. & ARIMA, Y. 2008 Self-motion of a phenanthroline disk on divalent metal ion aqueous solutions coupled with complex formation. *Colloids Surf.* A **324**, 222–227.

NAKATA, S., DOI, Y. & KITAHATA, H. 2004 Synchronized motion of a mobile boundary driven by a camphor fragment. *J. Colloid Interface Sci.* **279**, 503–508.

NAKATA, S., IGUCHI, Y., OSE, S., KUBOYAMA, M., ISHII, T. & YOSHIKAWA, K. 1997 Self-rotation of a camphor scraping on water: new insight into the old problem. *Langmuir* **13**, 4454–4458.

NAKATA, S. & KIRISAKA, J. 2006 Characteristic motion of a camphanic acid disk on water depending on the concentration of Triton X-100. *J. Phys. Chem.* B **110**, 1856–1859.

NAKATA, S., KIRISAKA, J., ARIMA, Y. & ISHII, T. 2006 Self-motion of a camphanic acid disk on water with different types of surfactants. *J. Phys. Chem.* B **110**, 21131–21134.

NAKATA, S., KOMOTO, H., HAYASHI, K. & MENZINGER, M. 2000 Mercury drop 'attacks' an oxidant crystal. *J. Phys. Chem.* B **104**, 3589–3593.

PAWAR, Y. & STEBE, K. J. 1996 Marangoni effects on drop deformation in an extensional flow: the role of surfactant physical chemistry. Part 1. Insoluble surfactants. *Phys. Fluids* **8**, 1738–1751.

PAXTON, W. F., KISTLER, K. C., OLMEDA, C. C., SEN, A., ANGELO, S. K. ST, CAO, Y. Y., MALLOUK, T. E., LAMMERT, P. E. & CRESPI, V. H. 2004 Catalytic nanomotors: autonomous movement of striped nanorods. *J. Am. Chem. Soc.* **126**, 13424–13431.

PAXTON, W. F., SUNDARARAJAN, S., MALLOUK, T. E. & SEN, A. 2006 Chemical locomotion. *Angew. Chem. Intl Ed.* **45**, 5420–5429.

PEDLEY, T. J. & KESSLER, J. O. 1992 Hydrodynamic phenomena in suspensions of swimming microorganisms. *Annu. Rev. Fluid Mech.* **24**, 313–358.

PHONGIKAROON, S., HOFFMASTER, R., JUDD, K. P., SMITH, G. B. & HANDLER, R. A. 2005 Effect of temperature on the surface tension of soluble and insoluble surfactants of hydrodynamical importance. *J. Chem. Engng Data* **50**, 1602–1607.

RAYLEIGH, L. 1890 Measurements of the amount of oil necessary in order to check the motions of camphor upon water. *Proc. R. Soc. Lond.* **47**, 364–367.

RUCKNER, G. & KAPRAL, R. 2007 Chemically powered nanodimers. *Phys. Rev. Lett.* **98**, 150603.

SCHILDKNECHT, H. 1976 Arthropod defense substances. Chemical ecology: a chapter of modern natural products chemistry. *Angew. Chem.* **15**, 214–222.

SCRIVEN, L. E. & STERNLING, C. V. 1960 Marangoni effects. *Nature* **187**, 186–188.

SNEDDON, I. N. 1966 *Mixed Boundary Value Problems in Potential Theory*. North-Holland.

SOH, S., BISHOP, K. J. M. & GRZYBOWSKI, B. A. 2008 Dynamic self-assembly in ensembles of camphor boats. *J. Phys. Chem.* B **112**, 10848–10853.

STONE, H. A. 1990 A simple derivation of the time-dependent convective-diffusion equation for surfactant transport along a deforming interface. *Phys. Fluids* **2**, 111–112.

TRIANTAFYLLOU, M. S., TRIANTAFYLLOU, G. S. & YUE, D. K. P. 2000 Hydrodynamics of fishlike swimming. *Annu. Rev. Fluid Mech.* **32**, 33–53.

TSAI, W. & YUE, D. K. P. 1995 Effects of soluble and insoluble surfactant on laminar interactions of vortical flows with a free surface. *J. Fluid Mech.* **289**, 315–349.

TSEMAKH, D., LAVRENTEVA, O. M. & NIR, A. 2004 On the locomotion of a drop, induced by the internal secretion of surfactant. *Intl J. Multiphase Flow* **30**, 1337–1367.

VOGEL, S. 1996 *Life in Moving Fluids*. Princeton University Press.

WANG, Z. J. 2005 Dissecting insect flight. *Annu. Rev. Fluid Mech.* **37**, 183–210.

YOUNG, N. O., GOLDSTEIN, L. S. & BLOCK, M. J. 1959 The motion of bubbles in a vertical temperature gradient. *J. Fluid Mech.* **6**, 350–356.